

Emergence of Artificial Photons in an Optical Lattice

Sumanta Tewari¹, V. W. Scarola¹, T. Senthil^{2,3} and S. Das Sarma¹¹Condensed Matter Theory Center, Department of Physics,
University of Maryland, College Park, MD 20742²Center for Condensed Matter Theory, Indian Institute of Science, Bangalore 560012, India³Department of Physics, Massachusetts Institute of Technology, Cambridge, Massachusetts 02139
(Dated: March 23, 2024)

We establish the theoretical feasibility of direct analog simulation of the compact U(1) lattice gauge theories in optical lattices with dipolar bosons. We discuss the realizability of the topological Coulomb phase in extended Bose-Hubbard models in several optical lattice geometries. We predict the testable signatures of this emergent phase in noise correlation measurements, thus suggesting the possible emergence of artificial light in optical lattices.

PACS numbers: 03.75.Lm, 03.75.Nt, 11.15.Ha

Introduction. Cold atomic gases in optical lattices [1] have provided unprecedented flexibility in designing and studying coherent and correlated condensed matter systems. To date, experiments on strongly correlated, bosonic lattice models have realized the on-site Hubbard-type interaction U , comparable to a nearest-neighbor hopping t . Consequently, several strongly correlated bosonic phases with short range interaction have been studied [2, 3, 4, 5]. However, with the recent observation of Bose-condensation of Chromium [6], which has a magnetic dipolar interaction, a sizable nearest-neighbor interaction V , albeit anisotropic, is now within experimental reach. Moreover, since U can be tuned using Feshbach resonances [7], $U=V$ can, in principle, be made to vary over a wide range. Furthermore, exciting developments [8] in cooling polar molecules offer the possibility of strong and tunable electrical dipole moments.

Recently, it has been proposed [9], that a four-site 'ring-exchange' interaction can also be implemented allowing the simulation of a U(1)-lattice gauge theory, which has various exotic topological phases, among them a 3D U(1) Coulomb phase with an emergent massless photon mode. In this Letter, we show that by simply implementing a Hubbard model with an additional strong nearest-neighbor interaction on some special lattices in both 2D and 3D one can efficiently simulate a U(1)-lattice gauge theory. The dipole interaction, $V_{dd}(R) = d^2 [1 - 3\cos^2(\theta)]/R^3$, where d characterizes the dipole moment and R is the inter-dipole separation, is, in general, anisotropic and depends on the angle between the vectors defining the parallel dipole orientation and the bond between the two dipoles. This interaction needs to be made isotropic for our purpose. This is easily done in 2D by simply aligning the dipoles perpendicular to the plane. In 3D, this is possible only on some lattice and we take the pyrochlore lattice where this can be achieved. Once the gauge theory is simulated, the Coulomb phase can be accessed by the appropriate tuning of interaction parameters. The existence of a gauge theory automatically implies that the conventional insulating phases [10]

are not the only phases possible.

We predict and discuss the observable signatures of the Coulomb phase, specifically, how the emergent photon mode, giving rise to artificial electrodynamics [11, 12, 13], can be detected in noise correlation measurements [14, 15, 16]. We note, in passing, that other fractionalized insulators of the gauge theory, where the elementary excitations carry fractional boson 'charge' (boson 'charge' in the present context of neutral bosons means boson number), can also be accessed in other regions of the parameter space. These, and experimental implications thereof, will be discussed in a future work [17].

Dipolar Bosons in Optical Lattices. We study the Coulomb insulating phase of dipolar bosons in optical lattices, specifically the Kagome (2D corner-sharing triangles) and pyrochlore (3D corner-sharing tetrahedra) lattices, see Fig. 1. Optical lattices formed from the intensity extrema of standing wave lasers can be used to generate a variety of lattices with non-trivial primitive unit cells using the superlattice technique [18], originally proposed to generate two dimensional lattices. Using this technique one can, in principle, generate a well defined set of intensity maxima defining the Kagome and the regular triangular lattices through angular interference of several beams with the same wavelength. Remarkably, the potentials defining these two lattices only differ by a phase. By generalizing this technique to three dimensions one can create a three-dimensional pyrochlore lattice by alternately stacking the triangular and Kagome lattices. Consider the following intensity pattern generated by counter-propagating, red-detuned lasers: $F_i(\mathbf{r}) = [\cos(\mathbf{k}_i \cdot \mathbf{r} + \phi_i) + 2\cos(\mathbf{k}_i \cdot \mathbf{r} + \phi_i + \pi/3)]^2$: With polarization (or frequency) mismatches, intensities can be added to generate the following three-dimensional potential with maxima defining a pyrochlore lattice: $V_p(\mathbf{r}) / \sum_{i=1}^5 B_i F_i(\mathbf{r})$: The relative intensities and wavevectors are given by: $B_{i6} = 1, B_4 = 2B_1, \mathbf{k}_1 = k(1; 0; -5/6), \mathbf{k}_{2,3} = k(1; -\sqrt{3}/2; 1/6),$ and $\mathbf{k}_5 = \mathbf{k}_4 = k(0; 0; 3/2)$. Here we have defined $4[1 - 2\cos^2(\theta)]^{1/2}$. The relative phases of the standing waves, $\phi_{i=2,4} = 0$ and

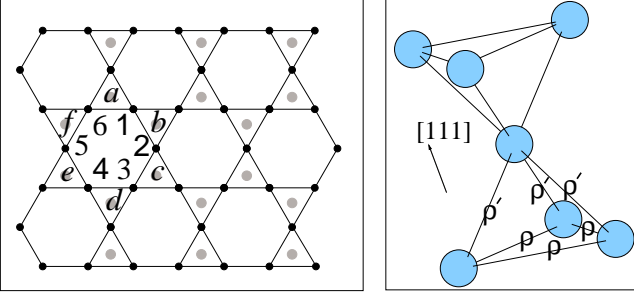


FIG. 1: In the left figure dipolar bosons sit on the sites of the 2D Kagome lattice, the black circles labeled 1-6. The hexagonal dual lattice, the lattice formed by the centers of the corner-sharing triangles (gray sites), is labeled a-f. In the right figure, for simplicity, we show only two corner-sharing tetrahedra of the pyrochlore lattice, with sites shown as spheres.

$\alpha_1 = \alpha_5 = \alpha_3 = 2$, must also be fixed. To generate V_p , we require phase matching between beams with varying spatial periodicities. The fact that the beams must also be tuned, energetically, to internal states of constituent bosons (which normally fixes the periodicity) poses an experimental challenge. However, recent experiments have in fact demonstrated multiple spatial periodicities through polarization-selective, angled interference [5] and Doppler-sensitive multi-photon transitions [19], separately. A combination of both techniques could offer a versatile system capable of realizing the standing wave arrangement used to produce V_p . Further details discussing the parameters and laser geometry for these lattices will be discussed elsewhere [17].

The interaction between dipolar bosons confined to optical lattices arises from two terms: the short range, s-wave, interaction, $V_s(R) = g^{(3)}(R)$, and the long range dipolar interaction $V_{dd}(R)$. In what follows we place the system in a uniform external field, pointing along the stacking direction (the [111] direction for the pyrochlore lattice) to orient the dipoles perpendicular to the basal plane. We also assume that the interaction strength g is tunable through Feshbach resonances, allowing tunability of the ratio $V_s = V_{dd}$. To make the dipolar interaction, $V_{dd}(R)$, isotropic we need a pyrochlore lattice where the tetrahedra are shrunk in the direction perpendicular to the basal plane, that is, $a_0 < a$, where a and a_0 are the tetrahedron side lengths within and out of the basal plane, respectively, see Fig. 1. The fact that the 3D nearest-neighbor interaction can be made isotropic along the bonds by such slight engineering of the tetrahedra is crucial, and so the pyrochlore lattice is the geometry of choice.

We now consider a simple model of dipolar bosons confined in deep optical lattices in the Hubbard limit. The resulting hopping term (tunable through the optical lattice depth) is nearest-neighbor while the interaction has both on-site and extended terms [10]. We omit

the smaller next-nearest neighbor interaction terms generated by the long range part of the dipolar interaction. Working in the insulating limit we may take the hopping energy gain (in units of the on-site energy) to be much smaller than the average number of particles per site. We then approximate the system by a quantum rotor model:

$$H = \sum_{\langle ij \rangle} t_{ij} b_i^\dagger b_j + \hbar \omega \sum_i n_i + U \sum_i n_i^2 + V \sum_{\langle \triangle \rangle} n_{\triangle} n_{\triangle}^0 : \quad (1)$$

Here $\langle ij \rangle$ denotes a nearest-neighbor pair of sites. $b_i^\dagger = \exp(i\phi_i)$ is the bosonic creation operator and $n_i = \phi_i^\dagger \phi_i$ counts the excess number of bosons at a site, i . The dominant contribution to U arises from the s-wave interaction while the dipolar interaction supplies the largest contribution to V . We assume that both U and V are large, and, in what follows, we will require U to be slightly larger than V . Here and in the following we omit the renormalized chemical potential term.

Mapping Onto Gauge Theory in 2D Kagome lattice. Eq. 1 can be written in a slightly different form more amenable to mapping onto a gauge theory. We take out a piece, $2U_0$, of the on-site interaction and group it together with V . Defining $N_{\triangle} = \sum_{i \in \triangle} n_i$ and $u = U - 2U_0$, we find, for $V = 2U_0$,

$$H = \sum_{\langle ij \rangle} t_{ij} b_i^\dagger b_j + \hbar \omega \sum_i n_i + u \sum_i n_i^2 + U_0 \sum_{\triangle} N_{\triangle}^2 : \quad (2)$$

Here, \sum_{\triangle} sums over all triangles in the lattice, and N_{\triangle} counts bosons on a given triangle. In this form, we call this Hamiltonian a 'cluster' Hubbard model where the fluctuations in the number of bosons on each local cluster (triangle) costs energy. This property enables a natural map to a gauge theory which enforces a local constraint.

Eq. 2 describes the same Hamiltonian as the one proposed before [11, 12] for a microscopic model of bosons on a square lattice and its 3D generalization, the corner-sharing octahedra. We focus here, however, on the Kagome lattice, for which the same Hamiltonian has an exact implementation in terms of a nearest-neighbor Hubbard model for $U = V$. The mapping of Eq. 2 on a $(2+1)$ -D U(1) lattice gauge theory is essentially the same as that on a square lattice. The details of the mapping, however, are different, which we briefly describe below.

A mapping onto gauge theory becomes possible when U_0 is the largest energy scale in the problem. The boson number on each triangle is then locally conserved. This implies $N_{\triangle} = 0$ on each triangle, meaning that the fluctuation in the boson number around the mean value set by the chemical potential vanishes. Working in the limit $U_0 \gg u$ and doing degenerate perturbation theory in t and u , we find, to first order in u and third order in t , the following effective Hamiltonian in the ground state sector $N_{\triangle} = 0$,

$$H_{\text{eff}} = u \sum_i n_i^2 - \frac{3t^3}{U_0^2} \sum_{\triangle} b_1^\dagger b_2^\dagger b_3^\dagger b_4^\dagger b_5^\dagger b_6 : \quad (3)$$

Here, \sum_{\triangle}^P sums over all hexagons inscribed in the triangles, and 1 through 6 indicate the corners of one such representative hexagon, see Fig. 1. This effective Hamiltonian is derived by locally conserving the number of bosons on each triangle. If a boson hops from site 6 to site 5, then another boson must hop from site 4 to site 3 to conserve the number of bosons on the triangle with one side defined by the bond (4-5), so that N_{\triangle} remains zero on that triangle. In turn, as is clear from Fig. 1, a third boson must hop from site 2 to site 1 to preserve the same constraint. Finally, since the u -term of Eq. 2 does not actuate N_{\triangle} , it comes in linear order in Eq. 3.

To see that this Hamiltonian exactly maps onto a lattice gauge theory on the dual lattice, we consider the dual lattice defined by the centers of the triangles. This is a hexagonal lattice whose sites we denote by $\mathbf{r}; \mathbf{r}^0$ etc. The original Kagome sites now fall on the links of the dual lattice. We take the representative hexagon, a through f , as shown in the left panel of Fig. 1, and identify the bosons on Kagome site l with the link (ab) etc.

On the dual lattice, by a change of notation, H_e reads,

$$H_e = u \sum_{\mathbf{r}; \mathbf{r}^0} n_{\mathbf{r}; \mathbf{r}^0}^2 - \frac{t^3}{U_0^2} \sum_{\triangle} b_{ab}^y b_{bc}^y b_{cd}^y b_{de}^y b_{ef}^y b_{fa}^y; \quad (4)$$

Next, noticing that the hexagonal lattice is bipartite, we define a field $a_{\mathbf{r}; \mathbf{r}^0} = a_{\mathbf{r}; \mathbf{r}^0}$ if $\mathbf{r} \in A$ and $\mathbf{r}^0 \in B$ and $a_{\mathbf{r}; \mathbf{r}^0} = a_{\mathbf{r}^0; \mathbf{r}}$ if $\mathbf{r} \in B$ and $\mathbf{r}^0 \in A$, where A and B are the two interpenetrating sublattices, and $b_{\mathbf{r}; \mathbf{r}^0} = \exp(i a_{\mathbf{r}; \mathbf{r}^0})$ as discussed after Eq. 1. We also define the conjugate field variable $e_{\mathbf{r}; \mathbf{r}^0} = n_{\mathbf{r}; \mathbf{r}^0}$ if $\mathbf{r} \in A$ and $\mathbf{r}^0 \in B$ and $e_{\mathbf{r}; \mathbf{r}^0} = n_{\mathbf{r}^0; \mathbf{r}}$ if $\mathbf{r} \in B$ and $\mathbf{r}^0 \in A$ (e and a are conjugate fields since n and a are). Finally, elevating a and e to vector fields $\mathbf{a}_{\mathbf{r}} = a_{\mathbf{r}; \mathbf{r}^+}$, $\mathbf{e}_{\mathbf{r}} = e_{\mathbf{r}; \mathbf{r}^+}$, where \mathbf{r}^+ indicates the nearest neighbor vectors, it is straightforward to see that H_e can be written as the Hamiltonian for the $(2+1)$ -D compact $U(1)$ gauge theory [20] on the dual lattice,

$$H_e = u \sum_{\mathbf{r}} e_{\mathbf{r}}^2 - \frac{t^3}{U_0^2} \sum_{\triangle} \cos(\mathbf{r} \cdot \mathbf{a}); \quad (5)$$

with the Gauss's law constraint $N_{\mathbf{r}} = N_4 = \sum_{\mathbf{r}^0 \in \triangle} n_{\mathbf{r}; \mathbf{r}^0} = \mathbf{r} \cdot \mathbf{e}$, and $\mathbf{r} \cdot \mathbf{e} = 1$ if $\mathbf{r} \in A$ and $\mathbf{r} \cdot \mathbf{e} = -1$ if $\mathbf{r} \in B$. We emphasize that Eqs. (4, 5) are simply rewritten forms of Eq. 3 on the dual lattice. Recall that a large U_0 implied the constraint on N_{\triangle} in Eq. 2 leading to Eq. 3. Hence, for an optical lattice implementation of the gauge theory, one simply needs to implement the Hamiltonian in Eq. 1 on appropriate lattices with both U and V large, with U slightly larger than V . The resulting low energy theory is automatically a gauge theory on the dual lattices, and so allows the exotic Coulomb phase and other fractionalized phases [11, 12, 20, 21] in addition to the conventional insulators [10]. In 2D, however, it is well known that the Coulomb phase is unstable at long length scales and is smoothly connected to the conventional Mott insulator.

Mapping Onto Gauge Theory in 3D pyrochlore lattice. We start with formally the same Hamiltonian as Eq. 1, but on a pyrochlore lattice. From Eq. 1, one straightforwardly gets the 'cluster'-Hubbard model, Eq. 2, with N_4 replaced by N_T , the number of bosons on a tetrahedron. The mapping to gauge theory on the dual diamond lattice, which is bipartite, but not Bravais, is identical and one ends up with Eq. 5 as the naive effective theory. To have a description of the dual lattice in terms of a Bravais lattice, we consider below only one FCC sublattice of the diamond lattice (centers of only one class of tetrahedra on the pyrochlore). Note that by counting the centers of only one class, and allowing an index to indicate all four corners of a tetrahedron from its center, we can count all the pyrochlore sites (diamond links).

In $(3+1)$ -D, the Coulomb phase, which is an insulator, is described by the Gaussian expansion of the cosine term of the gauge theory Hamiltonian, and is stable for $t \ll \frac{3}{4} u U_0^2$, since the topological defects { the monopole configurations of the gauge field } are suppressed in the Coulomb phase. This is analogous to the Gaussian expansion of the cosine term yields a Hamiltonian formally the same as that in classical electrodynamics, with an associated gapless photon mode. However, this is a gapless mode of the gauge field of the bosonic field operators, and not of an external electromagnetic field. This mode, which emerges in the low energy theory, should therefore be observable in the long-wavelength boson density-density correlation functions, and hence in noise correlations, given by the correlation functions of the e -fields (Recall that $e_{\mathbf{r}; \mathbf{r}^0}$ is simply related to $n_{\mathbf{r}; \mathbf{r}^0}$). This mode distinguishes itself from the conventional phonon mode resulting from spontaneously broken symmetry in strongly correlated, bosonic models because it appears in the absence of spontaneous symmetry breaking and is therefore an emergent phenomenon. Furthermore, this mode appears in a range of parameters ($U_0 \ll t \ll \frac{3}{4} u U_0^2$) intermediate between that for a superfluid ($t \ll U_0; u$) and the conventional insulators ($U_0; u \ll t$).

Noise Correlations in the Coulomb Phase. We now consider the long wavelength behavior of noise correlations in terms of the e -field correlation functions. To compute the correlation function of the e -fields, we work in the Coulomb gauge where $\mathbf{a} = 0$ and $\mathbf{r} \cdot \mathbf{a} = 0$. We then expand the cosine in the second term of Eq. 5 to quadratic order and use $e = \frac{\partial \mathbf{a}}{\partial t}$. Working in the continuum limit, the a -field correlator at momentum \mathbf{k} and (imaginary) frequency ω is given by,

$$\langle a_i(\mathbf{k}; i\omega) a_j(-\mathbf{k}; -i\omega) \rangle = \frac{ij}{\omega^2 + c^2 k^2} \frac{k_i k_j}{k^2}; \quad (6)$$

where $c^2 = (6t^3)/(uU_0^2)$. This reveals the mass-less

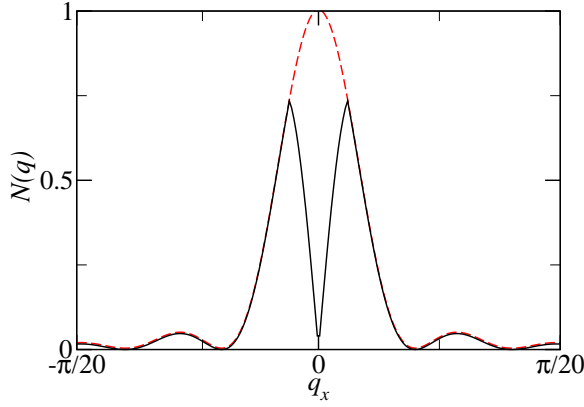


FIG. 2: Expected behavior of the normalized noise correlation function with q_x in the Mott insulating (dashed curve) and Coulomb (solid curve) phases around the first Brillouin-zone center of the FCC lattice. The core of the Mott insulating peak is suppressed due to the c_{ij} non-analyticity provided by the gapless 'photon' at long wavelengths in the Coulomb phase. The behavior, at large q , is expected to cross over to that of the Mott insulator. The plot is for a finite sized system with 100 sites along each direction with a small q slope $c = 40$ (with the appropriate form factor set to unity) and an arbitrarily chosen cut-off at $q_x = 3 = 500$.

emergent 'photon' mode. The equal-time correlator $\langle \mathbf{h}_r \cdot \mathbf{e}_{r^0} \cdot \mathbf{i} \rangle$, where \mathbf{i}, \mathbf{j}^0 are unit vectors for a tetrahedron, can be found from here. This gives the boson density-density correlation function. We find,

$$\langle \mathbf{h}_r \cdot \mathbf{n}_{r^0} \cdot \mathbf{i} \rangle = \langle \mathbf{h}_r \cdot \mathbf{e}_{r^0} \cdot \mathbf{i} \rangle = \frac{1}{i} \sum_j \langle \mathbf{h}_{ri} \mathbf{e}_{r^0 j} \rangle = \sum_j \sum_k c_{jk} \langle \mathbf{j} \cdot \mathbf{i} \rangle \frac{k_i k_j}{k^2} e^{i\mathbf{k} \cdot (\mathbf{r} - \mathbf{r}^0)} : (7)$$

A straightforward evaluation of this integral in the continuum gives the special angular structure of the Coulomb phase density correlation function at large distances [22]. However, as described below, for noise correlation, one is interested in the function in momentum space itself.

In time of light imaging of an insulating state of spinless particles, averaging the noise between shot-to-shot images of the particle distribution released from optical lattices reveals a quantity proportional to the following second order correlation function [14]:

$$N(\mathbf{q}) = \sum_{\mathbf{r}, \mathbf{r}^0} \sum_{\mathbf{i}, \mathbf{j}^0} e^{i\mathbf{q} \cdot (\mathbf{r} + \mathbf{r}^0 - \mathbf{i} - \mathbf{j}^0)} \langle \mathbf{h}_r \cdot \mathbf{n}_{r^0} \cdot \mathbf{i} \rangle; \quad (8)$$

where we, for simplicity, omit the $\mathbf{q} = 0$ delta function due to normal ordering. In a Mott insulator, which should be compared with the Coulomb insulator, $\langle \mathbf{h}_r \cdot \mathbf{n}_{r^0} \cdot \mathbf{i} \rangle$ is a constant, and so, for an infinite system $N(\mathbf{q}) = \sum_{\mathbf{q}_1} f(\mathbf{q}) f(\mathbf{q} - \mathbf{q}_1)$ where \mathbf{q}_1 's are the reciprocal lattice vectors of the FCC lattice, and $f(\mathbf{q})$ is the form factor of the tetrahedron basis, $f(\mathbf{q}) =$

$\sum_{\mathbf{i}, \mathbf{j}^0} \exp[i\mathbf{q} \cdot (\mathbf{r} - \mathbf{r}^0)]$. This produces δ -function peaks at the reciprocal lattice vectors which are the centers of the Brillouin zones. For the Coulomb phase, we know the behavior of $\langle \mathbf{h}_r \cdot \mathbf{n}_{r^0} \cdot \mathbf{i} \rangle$ only for large $|\mathbf{r} - \mathbf{r}^0|$. At smaller length scales, the calculation is quite involved since the full tetrahedron lattice correlators have to be used [17]. The long distance behavior, however, is sufficient to give the leading singularities at the Brillouin zone centers. From the integrand of Eq. 7 we see that, close to the zone centers, the leading singularity is a cusp, $N(\mathbf{q}) \sim |\mathbf{q}|^2$, see Fig. 2.

In conclusion, we have shown that compact U(1) lattice gauge theories can be simulated in suitably designed cold atom optical lattices using dipolar bosons. Exciting exotic phenomena, the Coulomb phase with emergence of artificial photons being an example, could be studied experimentally following our suggestion.

We thank L. Balents, H. Buchler, C. Zhang, A. Vishwanath and O. Motrunich for discussions. This research is supported in part by the National Science Foundation under Grant No. PHY99-07949, and ARO-DTO, ARO-LPS, and NSF. TS was very generously supported through a DAE-SRC Outstanding Investigator Award in India.

-
- [1] P. Verkerk et al, Phys. Rev. Lett. 68, 3861 (1992); P. S. Jessen et al, Phys. Rev. Lett. 69, 49 (1992); A. Hemmerich and T. W. Hansch, Phys. Rev. Lett. 70, 410 (1993).
 - [2] D. Jaksch et al, Phys. Rev. Lett. 81, 3108 (1998).
 - [3] M. Greiner et al, Nature (London) 415, 39 (2002).
 - [4] B. Paredes et al, Nature (London) 429, 277 (2004).
 - [5] J. Sebby-Strabley et al, Phys. Rev. A 73, 033605 (2006).
 - [6] A. Griemsmier et al, Phys. Rev. Lett. 94, 160401 (2005).
 - [7] M. Baranov et al, Physica Scripta T 102, 74 (2002); D. Jaksch and P. Zoller, Ann. Phys. (Berlin) 315, 52 (2004).
 - [8] Special issue on Ultracold Polar Molecules: Formation and Collisions, Eur. Phys. J. D 31 (2004).
 - [9] H. P. Buchler et al, Phys. Rev. Lett. 95, 040402 (2005).
 - [10] K. G. Gora et al, Phys. Rev. Lett. 88, 170406 (2002).
 - [11] T. Senthil and O. Motrunich, Phys. Rev. B 66, 205104 (2002).
 - [12] O. I. Motrunich and T. Senthil, Phys. Rev. Lett. 89, 277004 (2002).
 - [13] X. G. Wen, Phys. Rev. B 67, 245316 (2003).
 - [14] E. Altman et al, Phys. Rev. A 70, 013603 (2004).
 - [15] S. Foelling et al, Nature (London) 434, 481 (2005).
 - [16] I. B. Spielman et al, cond-mat/0606216.
 - [17] S. Tewari et al, unpublished.
 - [18] L. Santos et al, Phys. Rev. Lett. 93, 030601 (2004).
 - [19] G. R. Itt et al, cond-mat/0512018.
 - [20] J. B. Kogut, Rev. Mod. Phys. 51, 659 (1979).
 - [21] E. Fradkin and S. H. Shenker, Phys. Rev. D 19, 3682 (1979).
 - [22] M. Hermele et al, Phys. Rev. B 69, 064404 (2004).